The Astrophysical Journal, 767:61 (8pp), 2013 April 10 doi:10.1088/0004-637X/767/1/61

IN SEARCH OF DUST CLOUDS: PHOTOMETRIC MONITORING OF A SAMPLE OF LATE L AND T DWARFS

F. Girardin, É. Artigau, and R. Doyon
Département de Physique and Observatoire du Mont-Mégantic, Université de Montréal, C.P. 6128,
Succ. Centre-Ville, Montréal, QC, H3C 3J7, Canada; artigau@astro.umontreal.ca
Received 2011 September 19; accepted 2013 February 20; published 2013 March 25

ABSTRACT

Theoretical models indicate that L dwarf atmospheres are dominated by dust clouds made up of refractory elements; these clouds gradually disappear below the photosphere at the L/T transition. With the presence of dust-bearing clouds close to the photosphere, one expects weather-like features to appear on the brown dwarf surface, due to the presence of gaps in the cloud cover. We cannot hope to spatially resolve the disk of nearby brown dwarfs and directly explore the diversity of weather-like patterns on their surfaces with existing observational tools; therefore, indirect methods have to be used to probe these features, including rotation-induced flux modulation. In order to increase the sample of late L and T dwarfs probed for photometric variability, we observed a sample of nine brown dwarfs near the L/T transition. One target, SDSS J1052+4422 (T0.5), shows periodic flux variations with an evolving light curve and peak-to-peak amplitudes of ∼0.06 mag over a period of 3.0 hr, adding to the short list of early T dwarfs with semi-periodic photometric variability. The periodogram search also puts upper limits of ∼0.015 mag on the periodic variability of the remaining eight targets.

Key words: brown dwarfs – stars: individual (SDSS J105213.51+442255.7, SDSSp J125453.90−012247.4) – stars: low-mass – stars: variables: general – techniques: photometric

1. INTRODUCTION

The discovery of low-temperature, evolved, brown dwarfs (BDs) with spectral features not seen in stars led to the introduction of the new spectral classes of L dwarfs (2200–1300 K; Kirkpatrick et al. 1999; Martín et al. 1999), T dwarfs (1300 to <500 K; Kirkpatrick 2005; Leggett et al. 2005; Burgasser et al. 2006a) and, very recently, Y dwarfs (∼300 K; Cushing et al. 2011; Kirkpatrick et al. 2012). Although atmospheric models correctly predict the near-infrared (NIR) photometric properties of early L (*dusty* models) and late T (*clear* models) dwarfs, explaining the L/T transition, characterized by the so-called "*J*-band brightening" (Vrba et al. 2004; Burgasser et al. 2006b), remains a challenge to current models (Allard et al. 2003; Burrows et al. 2006; Helling et al. 2008).

A potential explanation for the *J*-band brightening is that some of these transition objects could be unresolved binaries (Burgasser et al. 2002a, 2006b; Liu et al. 2006). The apparent increase in binarity at the L/T transition can partially explain the *J*-band brightening especially for objects with the strongest brightening (Liu et al. 2006). However, the favored explanation is that the global cloud cover breaks up into discrete patches of clouds that eventually disappear below the photosphere by shrinking or sinking (Burgasser et al. 2002c; Marley et al. 2010). The inhomogeneous cloud cover could produce an observable photometric variability due to the rotation of the BD and/or the secular evolution of the cloud pattern. Showman & Kaspi (2012) provide a first semi-quantitative theory of the global circulation for BDs and find that large-scale temperature perturbations should indeed be expected near the photosphere of L/T transition objects.

Early BD variability studies focused mainly on optical variability of early L dwarfs, showing that many early L dwarfs exhibit brightness variations of a few percent in the *I* band on timescales ranging from hours to weeks (Tinney & Tolley 1999; Bailer-Jones & Mundt 1999, 2001; Terndrup et al. 1999; Martín et al. 2001; Clarke et al. 2002; Gelino et al. 2002; Maiti 2007). These brightness variations were found to be transient and rarely periodic. This suggests that they may not be due only to the rotational modulation of dust clouds but also to the rapid evolution of these features. Due to the low surface temperature of BDs, it is unlikely that the brightness variations are caused by mechanisms such as flaring (Burgasser et al. 2002b), accretion (Zapatero Osorio et al. 2003), or magnetic activity (Martín et al. 2001; Bailer-Jones et al. 2008).

There have been many observation campaigns to detect NIR variability in cooler dwarfs in recent years. Enoch et al. (2003) monitored nine BDs near the L/T transition using K_s-band photometry and reported relatively large variations (0.20–0.40 mag) with some evidence of periodicity (1.5–3.0 hr) on three targets. However, the targets were observed only a few times per night and the photometric uncertainties were relatively large (∼0.10 mag). Moreover, none of these variations could be confirmed by follow-up observations of the same targets by Koen et al. (2005). Koen et al. (2004) and Clarke et al. (2008), respectively, observed 18 and 8 dwarfs sampling the L/T transition with significantly smaller photometric uncertainties (∼0.01 mag in J, H, and K_s). While the data hint at some variability, there is no clear detection of periodic variations larger than 0.01 mag in the *J* band. Artigau et al. (2006) also searched for *J*-band variability on a sample of 10 L/T dwarfs and reported some marginal evidence of variability (∼0.05 mag; 1σ) on timescales of days but with no clear periodicity. Morales-Calderón et al. (2006) used *Spitzer* with the InfraRed Array Camera (IRAC) to monitor three late L dwarfs at mid-infrared wavelengths (4.5 μm and 8.0 μm) and, despite the remarkable photometric precision achievable with space-based observations (∼3–4 mmag), no unambiguous variability detection was reported with perhaps some marginal evidence of periodicity on 2MASS J2244+2043 (4.6 hr) and DENIS-P J0255−4700 (7.4 hr).

The discovery of correlated photometric variability in the J and K_s bands on the T2.5 dwarf SIMP0136 (Artigau et al. 2009) provides strong evidence for the presence of clouds on the surface of this BD. The observed periodic variability reaches a peak-to-peak amplitude of 0.050 mag in the *J* band with

Table 1
List of Selected Targets

Object Designation	Discovery Name	J	$J - K_s$	SpT[a]
2M0602	2MASS J06020638+4043588	15.544	0.378	T4.5
2M0727	2MASSI J0727182+171001	15.600	0.044	T7
SD0758	SDSS J075840.33+324723.4	14.947	1.068	T2
SD0805	SDSS J080531.84+481233.0	14.734	1.290	L9[b]
2M0937	2MASSI J0937347+293142	14.648	−0.619	T6
SD1052	SDSS J105213.51+442255.7	15.958	1.390	T0.5[c]
2M1106	2MASS J11061197+2754225	14.824	1.023	T2.5
SD1254	SDSSp J125453.90−012247.4	14.891	1.054	T2
2M1503	2MASS J15031961+2525196	13.937	−0.026	T5

Notes. Spectral types and photometric properties were drawn from the DwarfArchives.org online archive.
[a] SpT: infrared spectral type.
[b] Likely to be an unresolved spectroscopic binary: L4.5 + T5 (Burgasser 2007).
[c] Binary: T0.5 + T0.5 (Liu et al. 2010).

an unambiguous period of 2.388 hr. There is an even more spectacular example of a variable early T dwarf, as the T1.5 2M2139 was recently found to be variable with modulation amplitudes reaching ∼0.30 mmag (Radigan et al. 2012). The amplitude of photometric variability and the timescale for the evolution of the light curve observed for these two objects are in qualitative agreement with the BD atmospheric circulation models developed by Showman & Kaspi (2012).

Previous studies have clearly shown that photometric variability is not ubiquitous in BDs even for those near the L/T transition where one expects cloud patterns to emerge, but this result remains somewhat qualitative and needs to be confirmed by more observations and better statistics. This paper presents the results of a J-band variability search conducted on nine BDs with spectral types between L9 and T7. Section 2 presents the observation and data analysis techniques; Section 3 details the main results, which are discussed further in the context of other variability searches in Section 4.

2. OBSERVATIONS AND DATA REDUCTION

2.1. Sample Selection

The targets were selected from the BD archive database available from DwarfArchives.org. The sample was not constructed to be complete or unbiased in any way. Since atmospheric modeling suggests that photometric variability should be prominent in L/T transition objects (Marley et al. 2003), our targets were primarily chosen within this spectral-type domain but our sample also includes mid/late T dwarfs, one possible unresolved spectroscopic binary (SD0805; Burgasser 2007) and one equal-luminosity binary (SD1052; Liu et al. 2010). Another selection criterion was that the target should be visible for more than 4 hr continuously at an airmass less than 2.0 at the time of the observations. Finally, the sample was restricted to relatively bright sources ($J < 16$) to maximize the signal-to-noise ratio. Table 1 summarizes the properties of the nine targets observed.

2.2. Observations

The observations were made with the 1.6 m telescope of the Observatoire du Mont-Mégantic (OMM; Racine 1978) in southern Québec (Canada) between 2009 March 12 and 2010 May 24. Observations were obtained with the CPAPIR near-infrared camera (Artigau et al. 2004) featuring a 2048 × 2048 Hawaii-2 detector with a pixel scale of 0.″89 and a field of view (FOV) of 30′ × 30′. The detailed observation log is shown in Table 2.

Two observing strategies were used to obtain the light curves, namely staring and dithering. In staring mode, the target is kept at a fixed position on the detector with sub-pixel accuracy to minimize slight flat-field errors introduced by the intra-pixel response. However, the guiding probe was unable to keep a target perfectly fixed over a long period of time due to flexure between the probe and the telescope. Running an IDL script during the observations to provide real-time offset corrections solved this jitter problem. The telescope was also intentionally defocused to spread the point-spread function (PSF) of the target over more pixels and to reduce flat-field errors. The PSF FWHM was thus increased from its natural seeing value of 1″–2″ to about 3.″5. The exposure time was calculated for each target in order to optimize the signal-to-noise ratio while staying well within the linear range of the detector. The exposure times varied between 10 s and 30 s and exposures were co-added to get a frame rate of 1–2 minute^{-1}. The dithered observations were obtained by randomly moving the telescope by ∼20″ around the nominal position between each 20 s exposure. The seeing conditions varied between 1″ and 2″ for all nights.

These two strategies were attempted in order to compare their relative photometric accuracies; staring mode is becoming standard in very high accuracy NIR work (e.g., detection of secondary transits of exoplanets), while dithering is the more standard observing strategy for general-purpose NIR imaging. With the observing setup described above, and for targets in the $J = 14.0$–16.0 range, no significant difference was seen in the photometric precision achieved with these two methods.

The observations were carried out under a wide range of photometric conditions but only the data obtained in good conditions (no clouds except thin cirrus, seeing under 2″) were included in the analysis. A set of dome flats and darks were taken at the end of each night. The exposure time of the flats were set so as to accumulate enough photons to reach a pixel-to-pixel flat-field precision better than 1 part in 1000.

2.3. Data Reduction

All images were first processed with standard image reduction procedures consisting of subtracting the dark current, dividing by the flat field, and flagging bad pixels. For the dithered observations, the sky of each image was constructed by median-combining the five prior and five subsequent images with their stars masked. This method yielded a noticeably smaller background noise than in staring mode. Any residual background was then removed around every star by subtracting the median signal measured within an annulus with an inner diameter of 4 FWHM and an outer diameter of 8 FWHM. The stellar intensity was measured by integrating within a circular aperture with a diameter of 2 FWHM. This aperture size offers the optimal trade-off between the stellar signal and background noise contributions.

2.4. Comparison and Reference Stars

The flux of the target BD was normalized by that of an average reference star constructed by combining the flux of non-variable stars inside an 8′ radius. These reference stars were iteratively selected by keeping only those with small enough photometric uncertainties (final cutoff at 0.015 mag). Typically, over a dozen reference stars were retained to define the average reference signal. While there were many more stars available within the

Table 2
Observation Log

Object Designation	Observation Date	MJD[a]	Sequence Duration	Method
2M0602	2009 Oct 25	55130.694	4.9 hr	Dithering
	2009 Nov 1	55137.690	5.0 hr	Dithering
2M0727	2010 Mar 9	55265.527	4.5 hr	Dithering
SD0758	2010 Mar 10	55266.489	5.3 hr	Dithering
SD0805	2009 Mar 19	54910.540	2.2 hr	Staring
	2009 Mar 22	54913.529	3.2 hr	Staring
2M0937	2009 Mar 12	54903.574	1.9 hr	Staring
	2009 Mar 14	54905.496	3.3 hr	Staring
	2009 Mar 15	54906.509	3.4 hr	Staring
SD1052	2010 Mar 12	55268.607	5.6 hr	Dithering
	2010 Mar 15	55271.597	4.8 hr	Dithering
	2010 Mar 17	55273.501	4.0 hr	Dithering
	2010 May 23	55340.593	3.2 hr	Dithering
	2010 May 24	55341.652	1.9 hr	Dithering
2M1106	2010 Mar 11	55267.637	6.0 hr	Dithering
SD1254	2009 Mar 13	54904.681	5.3 hr	Staring
	2009 Mar 14	54905.656	4.9 hr	Staring
	2009 Mar 15	54906.670	5.7 hr	Staring
2M1503	2009 Mar 19	54910.650	6.8 hr	Staring
	2010 Mar 9	55265.796	3.6 hr	Dithering

Notes. [a] Modified Julian Date at the start of observations (MJD = JD−2 400 000.5).

Table 3
Photometric Precision

Designation	J (mag)	Duration[a] (hr)	Precision[b] (mmag)
2M0602	15.5	5, 5	12, 10
2M0727	15.6	5	11
SD0758	14.9	5	8
SD0805	14.7	2, 3	16, 10
2M0937	14.6	2, 3, 3	9, 6, 6
SD1052	15.9	6, 5, 4 3, 2	14, 20, 23 25, 24
2M1106	14.8	6	6
SD1254	14.9	5, 5, 6	7, 9, 6
2M1503	13.9	7, 4	3, 6

Notes.
[a] Each value corresponding to an individual night.
[b] Estimated from the average of 1σ error bars.

$30' \times 30'$ FOV of the camera, we decided to avoid stars near the edges of the FOV which could be more affected by systematic errors in the flat field due to optical distortion and large-scale illumination gradients.

3. RESULTS

3.1. Light Curves

Figure 1 shows a typical light curve for a non-varying target, 2M1106, while Figure 2 shows the light curve for the three first nights of monitoring of SD1052, which displayed significant, semi-periodic variability. Table 3 shows the photometric precision reached for all epochs and targets.

Table 3 shows the photometric uncertainty achieved for each night. Except for SD1052, the data do not show any short-term (a few hours) variability at the level (3σ) of a few tens of millimagnitude. However, as discussed in the following section, one can place tighter constraints on the amplitude of periodic variability.

Most targets have been observed on multiple nights. We normalized each night separately while preserving the same set of reference/comparison stars; we restricted our analysis to short-term variability as few constraints can be derived from night-to-night variations.

3.2. Periodograms

For each target and on each observation night, we built a Lomb–Scargle periodogram (Lomb 1976; Scargle 1982). To estimate the variability detection limits, Monte Carlo (MC) simulations were performed by randomly shuffling data points before constructing the periodograms. The 1σ, 2σ, and 3σ detection limits are fixed by finding the amplitude at which 68.3%, 95.4%, and 99.7% of the MC simulations yield smaller periodogram amplitudes. For each MC run, we performed 10^4 trials. SD1052 is the only target satisfying this criterion; a more detailed analysis of its periodograms is presented later. Figure 3 shows an example of a non-varying target (2M1106). Table 4 summarizes the 3σ variability limit of all targets and all observation nights.

3.3. SD1052

The periodogram search found statistically significant periodic variability for SD1052. There is clearly a significant peak around 3 hr and another one at half that period, which is interpreted as the second harmonic of the ∼3 hr signal. Although these periodogram peaks are present over more than one night, it is impossible to combine all nights as the relative phase

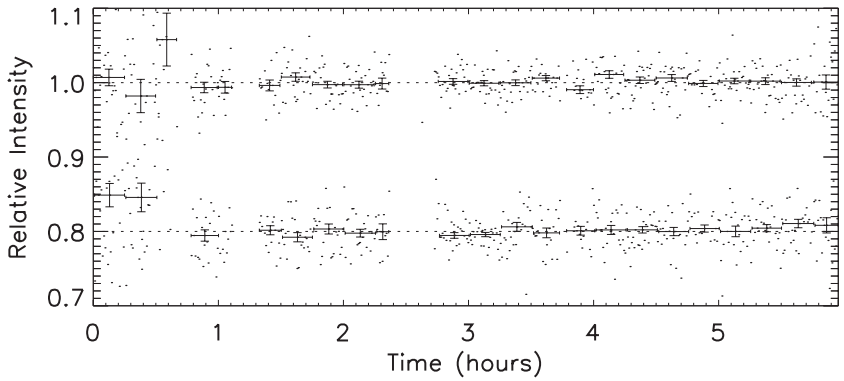

Figure 1. Representative light curve of a non-variable target, 2M1106, observed over 6 hr. Top: target; bottom: comparison star offset by −0.2. For both objects, dots represent individual photometric measurements and symbols with error bars represent 15 minute median flux. The uncertainty within each time bin is determined from a robust estimate of the standard deviation (IDL robust_sigma) within the bin divided by the square root of the number of measurements.

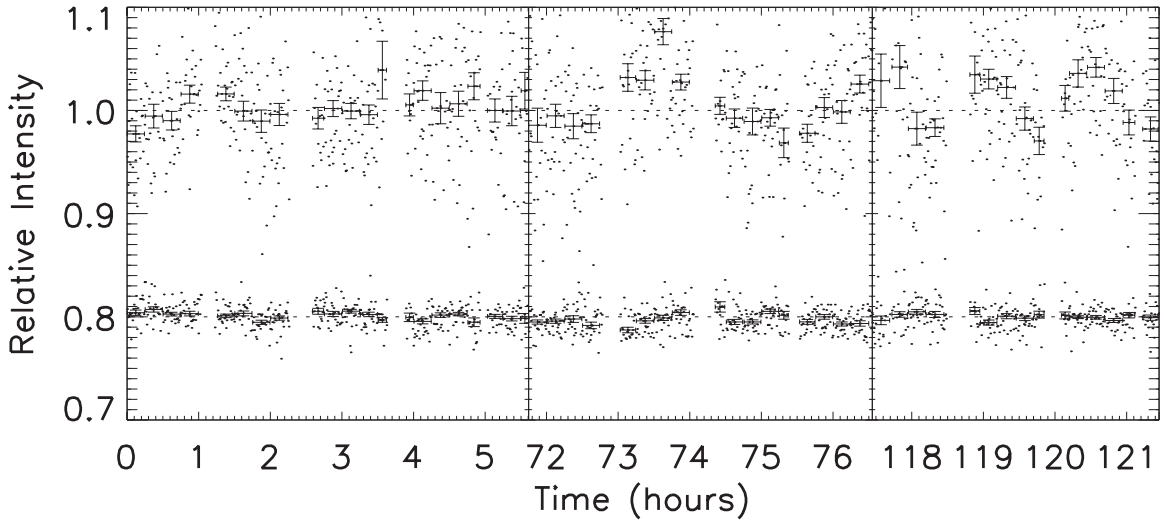

Figure 2. Light curve of SD1052 for the 2010 March 12–17 period. Significant variability is seen on all three nights; the semi-periodic behavior with a ∼1.5 hr period on the third night is clearly seen. Binned values and error bars are defined as for Figure 1.

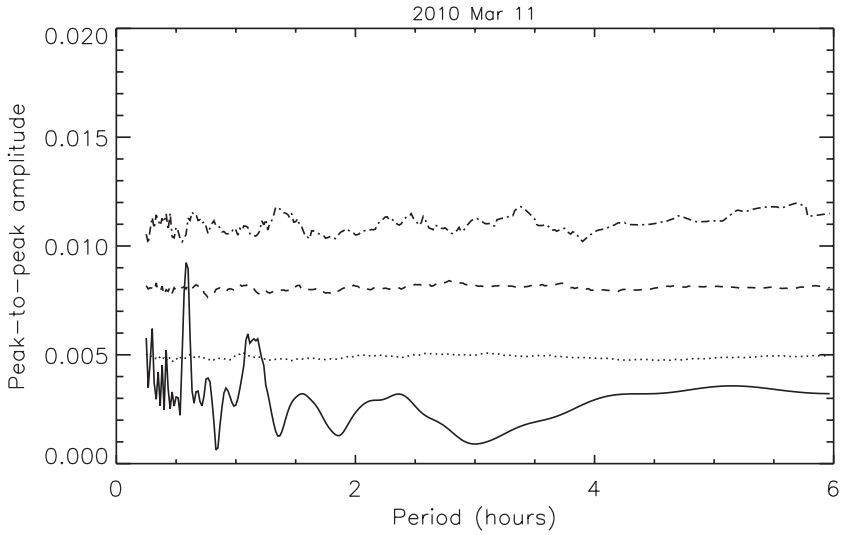

Figure 3. Periodogram of 2M1106 (solid curve) with its 1σ, 2σ, and 3σ detection limits plotted as a dotted line, a dashed line, and a dot-dashed line, respectively.

and amplitude of the first harmonic change between nights. Figures 4 and 5, respectively, show the periodogram and associated folded light curves for the three nights of monitoring in 2010 March and the two consecutive nights in 2010 May.

The periodic variability detected through our periodogram search is clearly seen in the phase-folded light curves shown in Figure 5, for the 2010 March 15 and March 17 data. For each of the epochs, we fitted the first and second harmonics and estimated the uncertainty on the fit through a MC simulation by

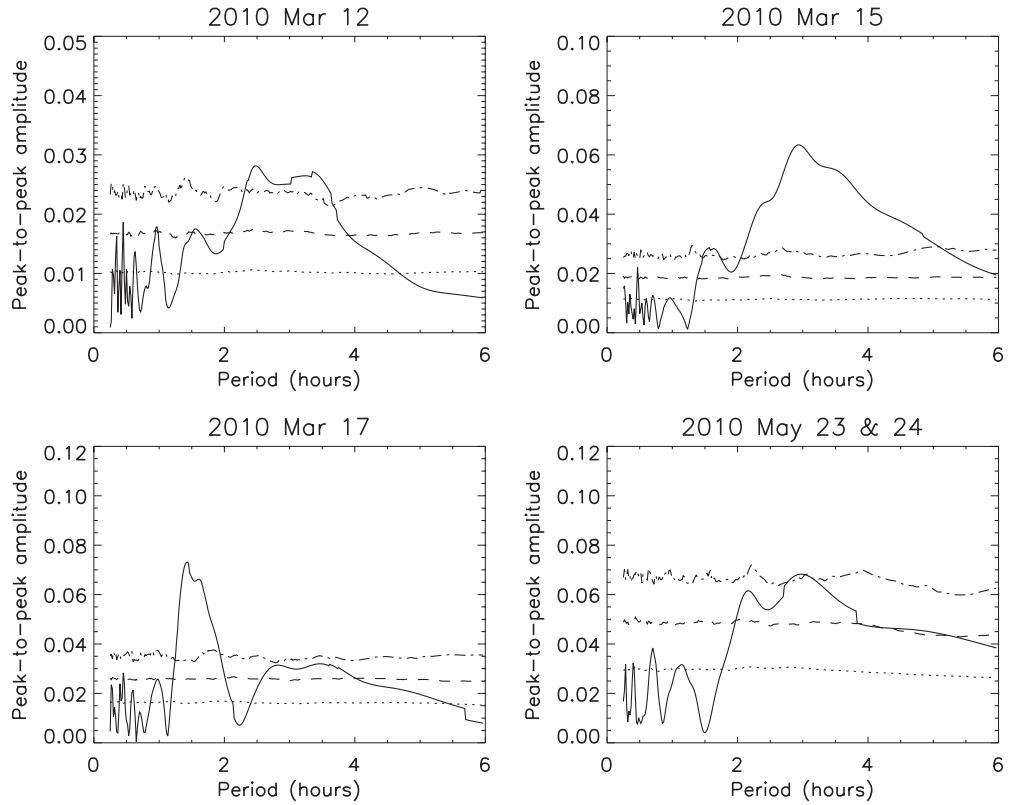

Figure 4. Periodograms of SD1052 (solid curve) with its 1σ, 2σ, and 3σ detection limits plotted as a dotted line, a dashed line, and a dot-dashed line, respectively. There is a significant peak (at or above the 3σ level) around 3 hr for all periodograms and a very strong peak around 1.5 hr on the 2010 March 17 periodogram. This peak is interpreted as the first harmonic of the 3 hr period.

Table 4
Periodic Variability Peak-to-Peak Amplitudes

Designation	Amplitude[a] (mmag)
2M0602	<9
2M0727	<13
SD0758	<9
SD0805	<12
2M0937	<6
SD1052	22–36
2M1106	<8
SD1254	<5
2M1503	<4

Note. [a] "<" indicates a 3σ upper limit for periods ranging from 1 to 6 hr.

Table 5
First and Second Harmonic Peak-to-peak Amplitudes for Four Photometric Time Series of SD1052

Night(s)	First Harmonic (mmag)	Second Harmonic (mmag)
2010 Mar 12	**25 ± 6**	16 ± 7
2010 Mar 15	**64 ± 8**	**28 ± 7**
2010 Mar 17	**29 ± 9**	**65 ± 9**
2010 Mar 23 and 24	41 ± 15	3 ± 10

Note. Detections above 3σ are shown in bold.

adding noise consistent with the point-to-point dispersion in the light curve. The results of this fit are reported in Table 5. The first harmonic is detected at the $>3\sigma$ level in three epochs and the second harmonic is detected in two of the four epochs. For both harmonics, the measured amplitudes between epochs are consistent with an evolving light curve; for example, the 2010 March 12 and March 15 amplitudes differ at the 4σ level.

4. DISCUSSION

A sample of nine BDs near the L/T transition was monitored photometrically in the *J* band. Each target was continuously observed for at least 4 hr over one or more nights. Eight of the nine targets showed no periodic variability above ∼0.01 mag. A single variable target, SD1052, was found, and it is one of the few known periodic variable BDs near the L/T transition (see Table 6).

The light curve of SD1052 shows, at least on two nights, two harmonics of varying relative amplitude. The presence of night-to-night variations in the light curve makes it impossible for the periodicity to be caused by a grazing binary, which would be strictly periodic, and thus reinforces the cloud cover hypothesis for the observed periodic variability. This argument against the presence of a (near-)contact binary has also been invoked for SIMP0136 and 2M2139, which also display an evolving periodic light curve (Artigau et al. 2009; Radigan et al. 2012). Our data set is too sparse to draw any firm conclusion regarding the geometry of clouds on SD1052, but tentative explanations can be explored. A single large dark or bright spot on the surface of the BD would lead to a nearly sinusoidal light curve, similar to the one observed for 2M2139. The presence of

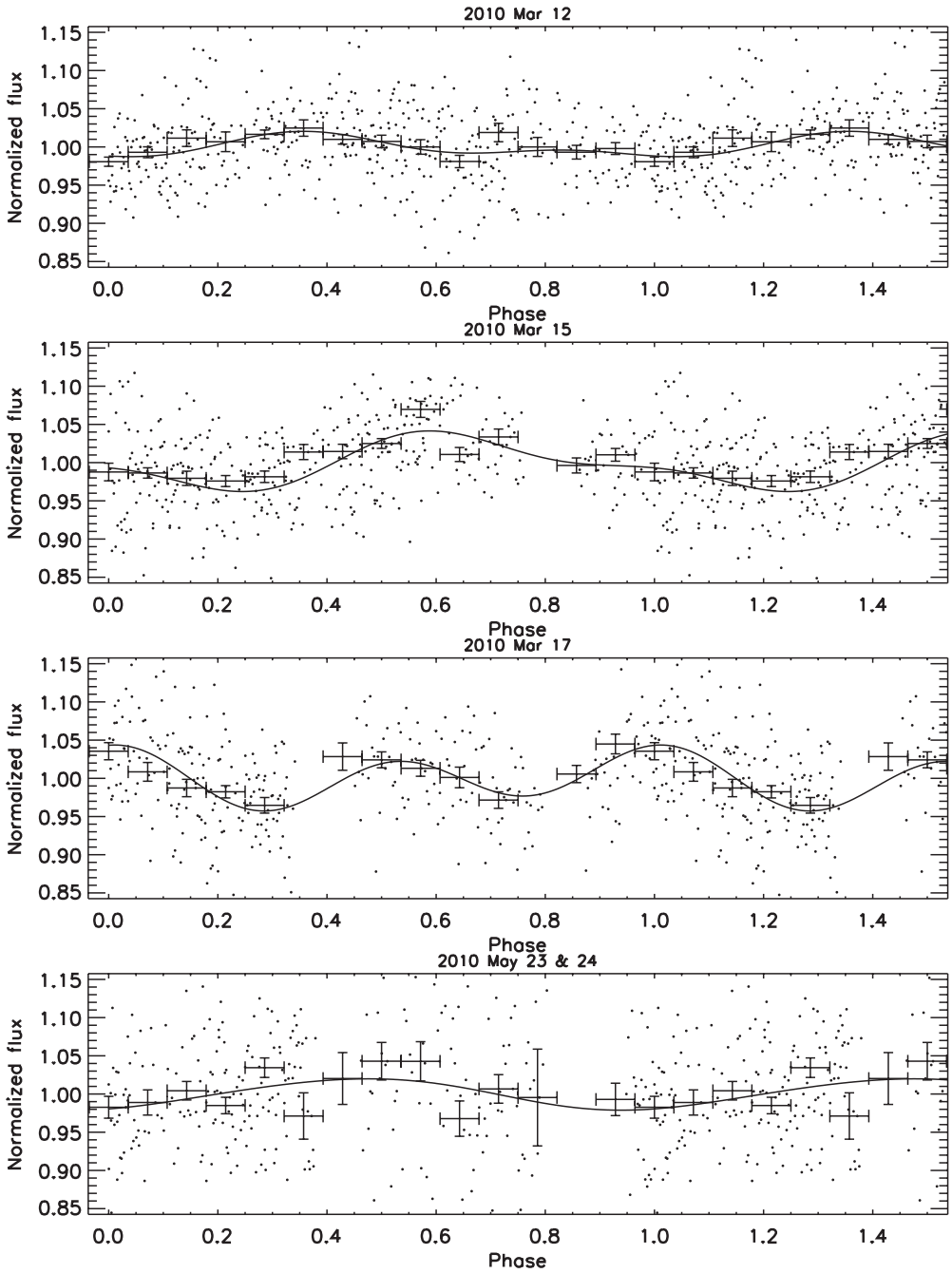

Figure 5. Light curves of SD1052 folded over the detected period of 3.0 hr. The overplotted line shows the best fit (first and second harmonics at an arbitrary phase). The relative phase of the light curves is arbitrary. Table 5 gives the measured peak-to-peak amplitude for both harmonics and for all epochs.

a strong second harmonic (e.g., data on 17 March 2010) can be tentatively explained if two similar-sized spots are present on opposite hemispheres of the object.

At the time of the observations, we were unaware that SD1052 is a tight binary (Liu et al. 2010), both components having a T0.5 spectral type. The binary is unresolved by our seeing-limited observations. Since variability near the L/T transition at the few percent level is relatively uncommon (∼10%), it is unlikely that both components are variable. Assuming that only one component exhibits variability would imply that the observed variability amplitude is diluted by a factor of two, which would put the intrinsic variability amplitude at about 10%, or between the values measured for SIMP0136 and 2M2139. The binarity of SD1052 does not affect our analysis of its variability but warrants more careful interpretation of the results.

As for the eight remaining targets, one can set strong upper limits on their short-term variability down to the ∼0.01 mag level. In turn, these variability limits yield some constraints on the presence of localized clouds/gaps in their atmosphere. Although there could be variations smaller than this detection limit, a non-detection might also be due to the rotation axis being oriented so as to keep the cloud/hole either behind or in front of the BD during its rotation. For randomly oriented spheres, this is a relatively unlikely scenario as only ∼5% of them are viewed within 20° of the poles so that periodic variability becomes undetectable. An inhomogeneous cloud cover could also be distributed in such ways that there is no rotational modulation

Table 6
Published *J*-band Variability for L6 or Later Objects

Publication	Variables >20 mmag	Variables <20 mmag	Number of Targets[a]
Koen et al. 2004	0[b]	1	8
Koen et al. 2005	0	0	5
Clarke et al. 2008	0	3	7
Artigau et al. 2009	1	0	1
Radigan et al. 2012	1	0	1
Buenzli et al. 2012	0	1[c]	1
Khandrika et al. 2013	3	0	6
This work	1	0	9
All	6	5	38

Notes. This compilation only includes *J*-band detections for which the variability detection threshold is below 0.02 mag. Overall, variability at the level observed for SIMP0136, 2M2139, and SD1052 would have been detected for all objects in this table.

[a] Khandrika et al. (2013), Koen et al. (2004, 2005), and Clarke et al. (2008) observed a larger number of targets, here we only count those meeting the criteria given in Section 4.1.

[b] ϵ Indi Bab is reported to be variable in *H* and *K* but does not have *J*-band measurements reported in this publication.

[c] 1.85% *J*-band variability derived from *Hubble Space Telescope* Wide-Field Camera 3 spectroscopy.

(e.g., longitudinal clouds). The variability could also be transient as suggested by the evolution of the light curves of SD1052, SIMP0136, and 2M2139.

Another target worth mentioning is the T2 dwarf SD1254 because it has been observed previously for the purpose of detecting photometric (Koen et al. 2004; Artigau et al. 2006) or spectroscopic (Goldman et al. 2008) variability. While the spectroscopic data do show some slight variations, the detection remains marginal and is not associated with any *J*-band variability. Koen et al. (2004) monitored SD1254 photometrically in the NIR and showed that SD1254 does not vary by more than 7, 6, and 10 mmag in the *J*, *H*, and K_s bands, respectively. These observations are consistent with the results presented in Table 4 showing that SD1254 does not vary periodically by more than 5 mmag in the *J* band. Therefore, SD1254 is not variable despite a spectral type and infrared color very close to those of SIMP0136. However, its level of variability could be changing significantly over timescales of months to years as suggested by the evolution of the light curve of variable early T dwarfs, justifying further monitoring of this target.

4.1. Fraction of Variable Late L and T Dwarfs in the J Band

Although models suggest that most BDs near the L/T transition may have inhomogeneous clouds, the low proportion of variable objects might be explained by the presence of mostly small-scale weather patterns greatly reducing the variability amplitude, while detectable, large-scale, inhomogeneities are rare and transient. Deriving the fraction of variable late L and T dwarfs from our sample and the literature is non-trivial as variability appears to be intermittent and published detection limits and time-sampling vary greatly through the literature. We attempt an order-of-magnitude estimate of the fraction of variable ultra-cool dwarfs by setting the following constraints: (1) only objects L6 and later are considered; (2) *J*-band photometric variability only is examined as variability level is color-dependent; (3) objects are considered only if the upper limits on their variability are below 0.02 mag peak-to-peak; and (4) an object is considered variable if the peak-to-peak amplitude is greater than 0.02 mag. Table 6 compiles the results of BD variability searches in the literature that meet the above criteria.

In the sample of 36 objects studied to date, 6 variable objects meet the above variability criteria while 4 others have significant, low-level variability (<0.02 mag). Note that some objects (e.g., 2M2139 in Radigan et al. 2012 and Khandrika et al. 2013) are counted more than once in the various publications; the values below should therefore be seen as a "per visit" likelihood of variability. One therefore has a ∼0.016 likelihood of detecting a >0.02 mag *J*-band variability in an L6+ dwarf over timescales of a few hours. It is important to keep in mind that 2M2139 has been found to be variable in a larger variability survey (J. Radigan et al. 2013, in preparation) and SIMP0136's variability has been identified in a single-target program that initially attempted to set strong upper limits on any non-variability. In a sense, neither can be seen as drawn from a statistically clean sample, so the above variability fraction should be seen as an order-of-magnitude estimate only. Furthermore, five additional targets (Clarke et al. 2008; Koen et al. 2004; Buenzli et al. 2012) display >3σ variability below the 0.02 mag limit, suggesting that a significant number of objects vary at the few mmag level. For example, the 8 mmag periodic variation of SD0423 found by Clarke et al. (2008) would have been below our detection threshold for all but three of our targets.

5. CONCLUSIONS

We have conducted a survey of photometric variability near the L/T transition and found that only one variable BD (SD1052; T0.5) out of a selected sample of L9-T7 dwarfs. SD1052 shows periodic variations with peak-to-peak amplitudes of ∼60 mmag (∼120 mmag when accounting for binarity) over a period of approximately 3 hr while the other eight targets do not display modulated variability at a level above 15 mmag on periods ranging from 1 to 6 hr. This sample is too small to put strong constraints on the fraction of variable BDs, but our observations, combined with published results from other variability surveys, suggest that the occurrence of *J*-band variability at the L/T transition is relatively modest, with roughly 9% of targets exhibiting peak-to-peak variability above 20 mmag. The evolution of the light curves of 2M2139, SIMP0136, and SD1052 on timescales of days indicates that atmospheric features are evolving quite fast. More observational data are needed to assess the prevalence of photometric variability among BDs near the L/T transition.

This research has benefited from the M, L, and T dwarf compendium housed at DwarfArchives.org and maintained by Chris Gelino, Davy Kirkpatrick, and Adam Burgasser.

Based on observations obtained with CPAPIR at the Observatoire du Mont Mégantic, funded by the Université de Montréal, Université Laval, the Natural Sciences and Engineering Research Council of Canada (NSERC), the Fond Québécois de la Recherche sur la Nature et les Technologies (FQRNT), and the Canada Economic Development program.

REFERENCES

Allard, N. F., Allard, F., Hauschildt, P. H., Kielkopf, J. F., & Machin, L. 2003, A&A, 411, L473
Artigau, E., Bouchard, S., Doyon, R., & Lafrenière, D. 2009, ApJ, 701, 1534
Artigau, É., Doyon, R., Lafrenière, D., et al. 2006, ApJL, 651, L57
Artigau, E., Doyon, R., Vallée, P., Riopel, M., & Nadeau, D. 2004, Proc. SPIE, 5492, 1479

Bailer-Jones, C. A. L., & Mundt, R. 1999, A&A, 348, 800
Bailer-Jones, C. A. L., & Mundt, R. 2001, A&A, 367, 218
Bailer-Jones, C. A. L., Smith, K. W., Tiede, C., Sordo, R., & Vallenari, A. 2008, MNRAS, 391, 1838
Buenzli, E., Apai, D., Morley, C. V., et al. 2012, ApJL, 760, L31
Burgasser, A. J. 2007, AJ, 134, 1330
Burgasser, A. J., Geballe, T. R., Leggett, S. K., Kirkpatrick, J. D., & Golimowski, D. A. 2006a, ApJ, 637, 1067
Burgasser, A. J., Kirkpatrick, J. D., & Brown, M. E. 2002a, ApJL, 571, L151
Burgasser, A. J., Kirkpatrick, J. D., Cruz, K. L., et al. 2006b, ApJS, 166, 585
Burgasser, A. J., Liebert, J., Kirkpatrick, J. D., & Gizis, J. E. 2002b, AJ, 123, 2744
Burgasser, A. J., Marley, M. S., Ackerman, A. S., et al. 2002c, ApJL, 571, L151
Burrows, A., Sudarsky, D., & Hubeny, I. 2006, ApJ, 640, 1063
Clarke, F. J., Hodgkin, S. T., Oppenheimer, B. R., Robertson, J., & Haubois, X. 2008, MNRAS, 386, 2009
Clarke, F. J., Oppenheimer, B. R., & Tinney, C. G. 2002, MNRAS, 335, 1158
Cushing, M. C., Kirkpatrick, J. D., Gelino, C. R., et al. 2011, ApJ, 743, 50
Enoch, M. L., Brown, M. E., & Burgasser, A. J. 2003, AJ, 126, 1006
Gelino, C. R., Marley, M. S., Holtzman, J. A., Ackerman, A. S., & Lodders, K. 2002, ApJ, 577, 433
Goldman, B., Cushing, M. C., Marley, M. S., et al. 2008, A&A, 487, 277
Helling, C., Ackerman, A., Allard, F., et al. 2008, MNRAS, 391, 1854
Khandrika, H., Burgasser, A. J., Melis, C., et al. 2013, AJ, 145, 71
Kirkpatrick, J. D. 2005, ARA&A, 43, 195
Kirkpatrick, J. D., Gelino, C. R., Cushing, M. C., et al. 2012, ApJ, 753, 156
Kirkpatrick, J. D., Reid, I. N., Liebert, J., et al. 1999, ApJ, 519, 802
Koen, C., Matsunaga, N., & Menzies, J. 2004, MNRAS, 354, 466
Koen, C., Tanabé, T., Tamura, M., & Kusakabe, N. 2005, MNRAS, 362, 727
Leggett, S. K., Allard, F., Burgasser, A. J., et al. 2005, in Proc. 13th Cool Stars Workshop, ed. F. Favata, G. A. J. Hussain, & B. Battrick (ESA SP-560; Noordwijk: ESA), 143
Liu, M. C., Dupuy, T. J., & Leggett, S. K. 2010, ApJ, 722, 311
Liu, M. C., Leggett, S. K., Golimowski, D. A., et al. 2006, ApJ, 647, 1393
Lomb, N. R. 1976, Ap&SS, 39, 447
Maiti, M. 2007, AJ, 133, 1633
Marley, M. S., Ackerman, A. S., Burgasser, A. J., et al. 2003, in IAU Symp. 211, Brown Dwarfs, ed. E. Martín (Cambridge: Cambridge Univ. Press), 333
Marley, M. S., Saumon, D., & Goldblatt, C. 2010, ApJL, 723, L117
Martín, E. L., Delfosse, X., Basri, G., et al. 1999, AJ, 118, 2466
Martín, E. L., Zapatero Osorio, M. R., & Lehto, H. J. 2001, ApJ, 557, 822
Morales-Calderón, M., Stauffer, J. R., Kirkpatrick, J. D., et al. 2006, ApJ, 653, 1454
Racine, R. 1978, JRASC, 72, 324
Radigan, J., Jayawardhana, R., Lafreni‘ere, D., et al. 2012, ApJ, 750, 105
Scargle, J. D. 1982, ApJ, 263, 835
Showman, A. P., & Kaspi, Y. 2012, arXiv:1210.7573
Terndrup, D. M., Krishnamurthi, A., Pinsonneault, M. H., & Stauffer, J. R. 1999, AJ, 118, 1814
Tinney, C. G., & Tolley, A. J. 1999, MNRAS, 304, 119
Vrba, F. J., Henden, A. A., Luginbuhl, C. B., et al. 2004, AJ, 127, 2948
Zapatero Osorio, M. R., Caballero, J. A., Béjar, V. J. S., & Rebolo, R. 2003, A&A, 408, 663